The scattering of SH waves by a finite crack with a superposition-based diffraction technique

CAMILO VALENCIA, JUAN GOMEZ, JUAN JARAMILLO, MARIO SAENZ AND JUAN VERGARA

Department of Civil Engineering, EAFIT University, Av. Las Vegas, 7sur 50, 05001000 Medellin, Colombia (cvalen20@eafit.edu.co)

Received: June 21, 2016; Revised: August 20, 2016; Accepted: August 24, 2016

ABSTRACT

The problem of diffraction of cylindrical and plane horizontally polarized shear waves (SH waves) by a finite crack embedded in a plane bidimensional elastic full-space is revisited. Particularly, we construct an approximate solution by the addition of independent diffracted terms. In our method the derivation of the fundamental case of a semi-infinite crack obtained as a degenerate case of a generalized wedge is first considered. This result is then used as a building block to compute the diffraction of the main incident waves. The interaction between the opposite edges of the crack is later considered in terms of a series, one term at a time until a desired tolerance is reached. Moreover, we propose a procedure to determine the number of required interactions as a function of frequency. The solution derived with the superposition technique is shown to be effective at low and high frequencies and as shown by comparisons with a direct boundary element method software, highly accurate solutions are obtained after retaining just a few terms of the infinite series.

Keywords: wave propagation, wave scattering, frequency domain analysis, diffraction, SH waves, SBD technique

1. INTRODUCTION

The determination of the scattered field produced by an elastic wave incident on a crack of finite length is of fundamental relevance in many different physics and engineering problems. For instance, cracks are frequently encountered at the interior of homogeneous media in the form of defects in machine parts (*Garnier et al., 2011*); as faults at the interior of the earth crust (*Murai, 2007*); or as cavities enclosing fossil energy reservoirs. In all of these cases, efficient engineering applications or understanding of related physical phenomena strongly relies on the level of accuracy and/or correct interpretation of the field scattered by a single crack. The study of the problem of diffraction by a single crack is also of paramount and fundamental importance in understanding the response of complex problems. For instance, *Sánchez-Sesma and Iturrarán-Viveros (2001)* highlight the importance of the single crack problem in the particular case of densely cracked media when the radii of separation between cracks is small compared to the wavelength and as a result the interaction between cracks is

negligible. As stated by these authors, in such cases it is important to differentiate diffraction patterns caused by many cracks from that of a single crack.

This paper considers the well known problem of scattering and diffraction of horizontally polarized *SH* waves caused by a crack of finite length placed in the interior of an isotropic elastic two-dimensional (2D) full-space. We derive an approximate solution in the cases where the crack is impinged on by either a plane or a cylindrical *SH* wave. Our solution is built using the superposition of fields contributed by different diffraction sources emanating from a generalized wedge. Although the solution takes the form of an infinite series, high accuracy can be obtained after retaining just a few terms, each one of which represents the contribution from a diffraction source. Our solution differs from previous ones, found in the literature, in the fact that the diffracted field is obtained directly within a single analysis step which allows us to obtain the near and far field response by a simple procedure.

The problem of scattering of plane *SH* waves by cracks has been widely studied from a numerical and an analytical point of view. A review of seminal works on this subject can be found in *Mow and Pao (1971)* and *Achenbach et al. (1982)*. A landmark contribution to the problem is the closed-form solution developed by *Sommerfeld (1896)* in the case of *SH* waves impinging upon a semi-imfinite crack. A solution in the time domain was also developed by *De Hoop (2000)*. That author derived a closed-form expression for the scattering of a plane *SH* wave introduced by a generalized linear slip fracture of finite length in the Kirchhoff approximation. Similarly, *Caleap et al. (2007)* found an analytic expression for the angular function proposed by *Waterman and Truell (1961)* in order to describe the far field scattered by a single crack. In more recent contributions the problem was also solved by *Tsaur (2010)* using a region matching technique leading to a series solution with the terms corresponding to eigenfunctions and *Chen et al. (2013)* who used a set of boundary integral equations, while recent numerical approaches based upon direct (and indirect) boundary element method formulations and finite difference schemes are discussed in *Iturrarán-Viveros et al. (2005)*, *Pérez-Ruiz et al. (2007)* and *Chen et al. (2012)*.

Works dealing with semi-infinite cracks as particular instances of generalized, semi-infinite wedges led to a number of studies for crack problems, see for instance *MacDonald (1902)*, *Hudson (1963)* and *Abo-Zena and King (1973)*. The solution to the semi-infinite crack is relevant since it allows the representation of a finite crack as the superposition of two semi-infinite cracks. For instance, following that approach *Sánchez-Sesma and Iturrarán-Viveros (2001)* performed a superposition of *Sommerfeld (1896)* solution and found an expression for the diffracted field produced by a plane *SH* wave incident upon a single crack of finite size. In that solution, the cylindrical waves resulting from the diffraction of the primary incident plane wave front as it interacted with the edges, were limited to propagate as plane waves before interacting with the opposite edge. The same solution approach was later extended by *Iturrarán-Viveros et al. (2010)* to the case of incident cylindrical waves. Both solutions have been frequently used by various authors as a benchmark problem for the validation of numerical tools (*Krüger et al., 2005*). Our solution is strongly related to the work by *Sánchez-Sesma and Iturrarán-Viveros (2001)* and *Iturrarán-Viveros et al. (2010)* in the manner in which we separate the fields. However, in our approach we accurately consider the interaction between the crack edges in terms of cylindrical fronts; we find the near and far field response by a simple to

apply procedure. Most importantly, the accuracy of the solution is controlled after retaining just a few terms corresponding to diffracted waves.

The idea of separating the total field in a wedge into terms related to the incident, reflected and diffracted displacements has already been explored in the geometrical theory of diffraction (GTD) by *Keller (1957, 1956, 1962)* and later improvements by *Kouyoumjian and Pathak (1974)*, who represented the diffracted field for a generalized wedge under incident plane and cylindrical fronts in terms of diffraction coefficients similar to those used in the solution of reflection-transmission problems. In this work we follow that superposition-based approach, using a technique recently proposed by *Jaramillo et al. (2013)* to deal with problems involving *SH* waves interacting with free surfaces of arbitrary shape. It must be pointed out that in principle the superposition-based diffraction (SBD) technique is applicable to problems involving free surfaces of arbitrary shape. However, when there is a large number of interacting diffraction sources, the efficiency of the solution method decreases unless it is properly implemented in a computer code. In any case, our proposed solution contributes to the conceptual understanding of the problem improving at the same time the interpretation of results from numerical algorithms.

That so-called SBD approach uses the wedge solution from *Kouyoumjian and Pathak (1974)* as a fundamental building block and then proceeds as in *Sánchez-Sesma and Iturrarán-Viveros (2001)*, where the finite crack is obtained as the superposition of two semi-infinite cracks. Here we first describe the canonical solution by *Kouyoumjian and Pathak (1974)*, corresponding to the diffraction of electromagnetic waves by a generalized wedge. That solution is subsequently used to derive the contribution from the diffracted field which is used to build the solution to the diffraction by a finite crack after its recursive application in terms of primary and higher order diffraction terms. The obtained solution, valid for cylindrical and plane waves, is then simplified and the focus directed to the case of normal incidence. Since the proposed solution takes the form of an infinite series, we present a recipe to determine the number of terms required to adequately approximate the actual solution, using as inputs the amplitude and frequency of the incident wave and a predefined tolerance. In order to validate our solution to the crack problem, we compare frequency and time domain results with those obtained using an integral equation representation in terms of the Somigliana identity. We show that accurate solutions are in fact obtained with just a few terms in the series.

2. DIFFRACTION BY A SEMI-INFINITE CRACK AS A PARTICULAR INSTANCE OF THE DIFFRACTION BY A GENERALIZED WEDGE

In this section we describe for completeness the canonical problem forming the basis of the SBD technique formulated in *Jaramillo et al. (2013)*. The problem domain and incident wave field are defined in Fig. 1. It consists of a generalized wedge with perfectly reflecting surfaces intercepting at an edge singularity of external angle $\nu\pi$, where ν is a factor that completely defines the wedge and varies between 0.0 and 2.0. The generalized wedge is impinged upon by an incident plane wave front defined by its propagation direction (forming an angle ϕ' with the free surface of the wedge). In Fig. 1,

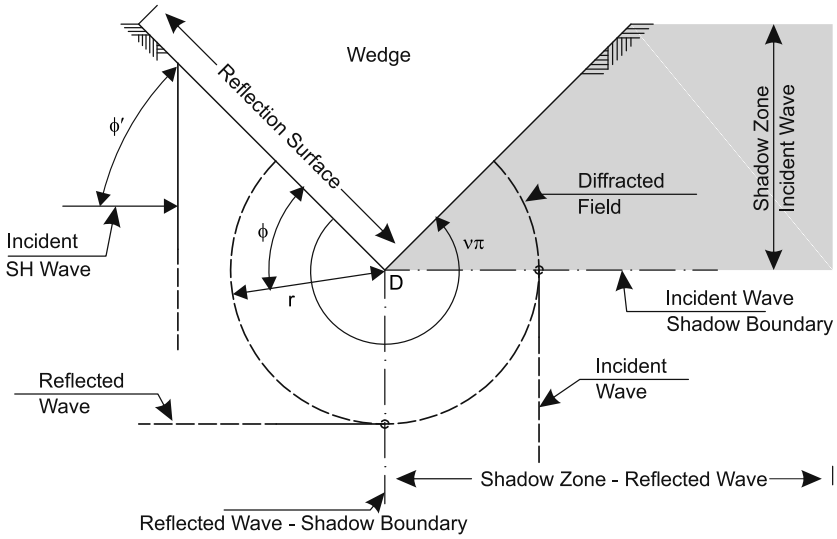

Fig. 1. Plane wave incident on a generalized wedge.

regions of existence (or absence) of incident and reflected rays are fully described. Here we follow the common terminology of the geometrical theory of diffraction and refer to these regions as illuminated or shadow zones.

The lines separating the different regions of existence of incident and reflected rays, and denoted in the figure as reflection and incidence boundaries, represent regions of discontinuity of each term considered independently. The diffraction field generated by the edge singularity corresponds to a cylindrical wave that penetrates into the shadow zone and restores continuity along these reflection and incidence boundaries. In summary, the construction process to find the solution for a single wedge amounts to finding the total field contributed by the incident (w^{inc}) and reflected (w^{r}) fields, which are discontinuous or even absent from certain regions; plus the consideration of the diffracted field w^{D} generated at the edge singularity and restoring continuity everywhere, i.e., the term w^{D} provides the proper transition between the illuminated and the shadow zones.

In the SBD approach, the contribution of the diffracted field is taken directly from the approximate solution proposed by *Kouyoumjian and Pathak (1974)* and corresponding to a generalized infinite wedge submitted to an incident plane or cylindrical wave. The generalized solution for the diffracted field is given in Eq. (1) for a field point with coordinates (ϕ, r) as follows

$$w^{D}(\phi, r) = A^{inc} G(\phi, \phi', r, L) \ , \tag{1}$$

where

$$G(\phi,\phi',r,L)=\frac{-e^{\left[-i(kr+\pi)/4\right]}}{2\nu\sqrt{2\pi}\sqrt{kr}}\left[\cot\left(\frac{\pi+(\phi-\phi')}{2\nu}\right)F\left(kLb^{+}(\phi-\phi')\right)\right.$$
$$+\cot\left(\frac{\pi-(\phi-\phi')}{2\nu}\right)F\left(kLb^{-}(\phi-\phi')\right)+\cot\left(\frac{\pi+(\phi+\phi')}{2\nu}\right)F\left(kLb^{+}(\phi+\phi')\right)$$
$$\left.+\cot\left(\frac{\pi-(\phi+\phi')}{2\nu}\right)F\left(kLb^{-}(\phi+\phi')\right)\right].$$

A^{inc} is the amplitude of the incident wave at the edge, r is the radial coordinate to the field point measured from the vertex of the wedge, ϕ is the angular coordinate measured with respect to the reflection surface, ϕ' is the incidence angle measured with respect to the reflection surface, $\nu\pi$ is the wedge angle with $0.0 \le \nu \le 2.0$, k is the angular wave number, and $i=\sqrt{-1}$. The remaining terms appearing in Eq. (1) are defined as

$$F(X)=2i\sqrt{X}e^{iX}\left[\sqrt{\frac{\pi}{8}}(1-i)-\sqrt{\frac{\pi}{2}}\left(C\left(\sqrt{X}\right)-iS\left(\sqrt{X}\right)\right)\right],$$

$$L=r \quad \text{for incident plane waves,}$$

$$L=\frac{rr'}{r+r'} \quad \text{for incident cylindrical waves,}$$

$$b^{\pm}(\theta)=2\cos^2\left(\frac{2\nu\pi Z^{\pm}-\theta}{2}\right),$$

$$Z^{+}=\begin{cases}0 & \text{if} \quad \theta\le\nu\pi-\pi,\\ 1 & \text{if} \quad \theta>\nu\pi-\pi,\end{cases} \quad Z^{-}=\begin{cases}-1 & \text{if} \quad \theta<\pi-\nu\pi,\\ 0 & \text{if} \quad \pi-\nu\pi\le\theta\le\pi+\nu\pi,\\ 1 & \text{if} \quad \theta>\pi+\nu\pi,\end{cases}$$

with $C(\bullet)$ and $S(\bullet)$ being the Fresnel integrals, r' is the radius of the incident cylindrical wave (for the diffraction of a cylindrical front),

From the solution described above it is clear that the contribution from the diffraction source is a cylindrical front and that for values of ϕ corresponding to points far removed from the incidence and reflection boundaries, the amplitude from that front decays as $1/\sqrt{kr}$. On the other hand, right at the incident/reflection boundary the diffracted field is discontinuous. This is a required condition that must be satisfied by the term w^D in order to match the corresponding discontinuity appearing in the superposition of the incident and reflected contributions.

3. DIFFRACTION BY A FINITE CRACK VIA SUPERPOSITION OF DIFFRACTION SOURCES

3.1. Arbitrary incidence

In order to obtain the solution for the diffraction of incident *SH* waves by a single crack we start from the solution to the problem already shown in Fig. 1 (see Eq. (1)). If the angular factor ν is given the particular value of 2.0, the generalized wedge collapses into a zero-thickness semi-infinite crack with traction free surfaces. Two such cracks, defined in $y \in (-\infty, a/2]$ and $y \in [-a/2, \infty)$ can then be superimposed to yield a single crack of length $l = a$ defined by the domains of intersection of the two fundamental cracks; i.e., in $y \in [-a/2, a/2]$. The above superposition scheme and the specific parameters that must be applied in Eq. (1) in order to consider incidence of plane and cylindrical fronts is described in Fig. 2.

Following the SBD approach we have that in the most general case the total solution w^T can be built from the superposition of an incident field w^{inc}, a reflected field w^r and a contribution from the diffraction sources w^D according to;

$$w^T = w^{inc} + w^r + w^D . \tag{2}$$

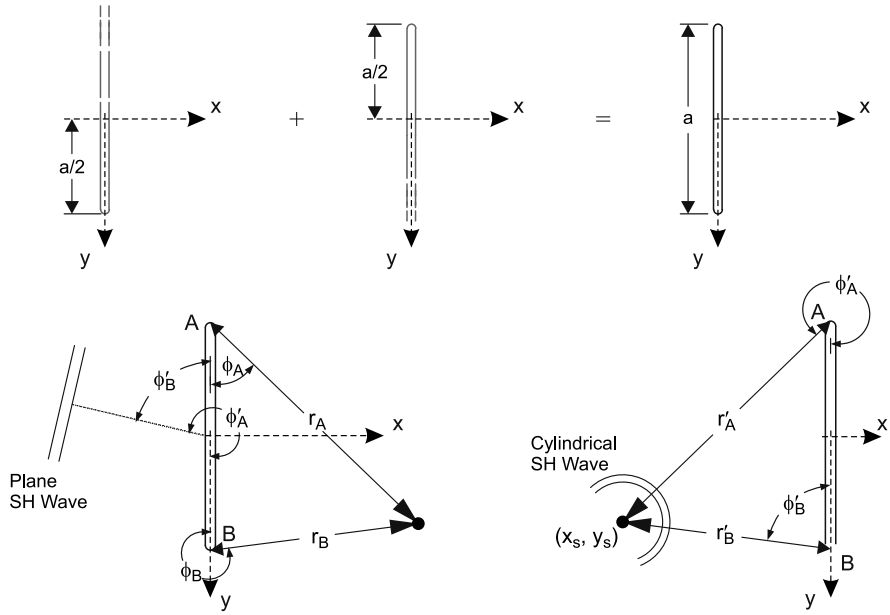

Fig. 2. Problem definition and construction of the solution for a finite crack using the superposition of fundamental semi-infinite cracks.

In the particular case of an incident plane wave, the term w^{inc} is given by:

$$w^{inc} = w_0 \mathrm{e}^{\mathrm{i}kx\sin(\phi'_B)+\mathrm{i}ky\cos(\phi'_B)},$$

while for a cylindrical wave this field corresponds to:

$$w^{inc} = \frac{w_0}{\sqrt{\hat{R}}}\mathrm{e}^{\mathrm{i}kR},$$

where $\hat{R} = R/R_0$, R is the distance measured from the source point (x_s, y_s), R_0 = 1.0 km, and w_0 is the amplitude at R_0. In the proposed solution technique the incident and reflected fields are obtained in closed form, while the contribution from the diffracted field is approximated since it is represented by a finite number of terms. This approach is in contrast to those based upon eigenfunction expansions of the total field. In the current method on the one hand, the terms corresponding to the incident and reflected fields are known beforehand and thus not need to be represented in the series, while in the other hand the geometric irregularity not need to be limited to a shape where separation of variables can be applied.

After removing for simplicity the D superscript denoting the diffraction terms in Eq. (2) it follows that the solution in the illuminated zone takes the form:

$$w^T = w^{inc} + w^r + w_A + w_B + w_{AB} + w_{BA} + w_{ABA} + w_{BAB} + \dots \ . \tag{3}$$

Similarly, in the zone where the reflected field is absent, the solution is given by

$$w^T = w^{inc} + w_A + w_B + w_{AB} + w_{BA} + w_{ABA} + w_{BAB} + \dots \ , \tag{4}$$

and finally, in the shadow zone, the solution has the form

$$w^T = w_A + w_B + w_{AB} + w_{BA} + w_{ABA} + w_{BAB} + \dots \ . \tag{5}$$

In the expressions above we have introduced subscripts to indicate diffraction events. For instance, the terms w_A and w_B represent the contributions from the diffraction experienced by the initial incident wave front as it interacts with the edges of the crack. Similarly, in a term like w_{BABA} in the same equation, the first B-subscript indicates that the incident wave experienced diffraction by the edge B generating a cylindrical front which is subsequently diffracted at the opposite edge A, generating a secondary cylindrical front, which is diffracted again at the edge B and once again at the edge A. Accordingly, the number of subscripts in each term represents the number of diffraction events experienced by the initial incident wave front.

The different terms in the series are obtained after the recursive application of Eq. (1) with first order contributions corresponding to the main plane or cylindrical fronts, according to the considered case, but with second and higher order contributions always representing cylindrical fronts. This consideration of the diffracted waves as true cylindrical fronts is one of the differences between our solution and the one derived in *Sánchez-Sesma and Iturrarán-Viveros (2001)*, where the diffracted field is assumed as composed of plane waves before considering its second order diffraction by the opposite edge.

After some mathematical manipulations the final solution for the diffracted field can be written as

$$w^D\left(\phi_A, \phi_B, r_A, r_B\right) = w_A^{inc} \sum_{n=1}^{N} V_A G\left(\phi_A, \phi_A', r_A, L_{A,n}\right) + w_B^{inc} \sum_{n=1}^{N} V_B G\left(\phi_B, \phi_B', r_B, L_{B,n}\right), \tag{6}$$

where the required terms are defined in the Appendix. The number of terms N after which the series is truncated, clearly corresponds to the number of considered diffraction events in the solution. It is clear that the exact solution is attained in the limit when $N \to \infty$. However, since each term in the series corresponds to a diffraction event represented by a cylindrical front whose amplitude decreases with respect to the one in its parent wave, accuracy is controlled in terms of the number of diffraction events. This relation between the number of terms appearing in the series and the number of diffraction sources allows the solution to be extended to any desired accuracy depending on the value of the dimensionless frequency parameter $\eta = a/\lambda$ relating the crack length to the incident wave length.

3.2. Normal incidence at $\phi_B' = \pi/2$

In the particular case of normal incidence (i.e., $\phi_B' = \pi/2$) and due to the geometric symmetry of the problem, terms like w_A^{inc} and w_B^{inc} in Eq. (6) take equivalent values. Thus the diffracted field simplifies to

$$w^D\left(\phi_A, \phi_B, r_A, r_B\right) = w_A^{inc} \sum_{n=1}^{N} \left\{ \left[\frac{-\mathrm{e}^{-\mathrm{i}(ka+\pi/4)}}{2\sqrt{\pi ka}} F(ka) \right]^{n-1} \left[-G\left(\phi_A, r_A, L_{A,n}\right) + G\left(\phi_B, r_B, L_{B,n}\right) \right] \right\}. \tag{7}$$

Once again the parameter N limiting the series depends on the value of the dimensionless frequency η and the pre-established level of accuracy. At larger values of η, relatively small values of N are required. Physically, this means that at larger values of η the solution corresponding to a desired accuracy is achieved with fewer diffraction orders.

3.3. A recipe to determine the diffraction order N required for a predefined tolerance

We now propose a procedure that can be used to estimate the number N of diffraction orders that must be considered in Eq. (6), given a value of the dimensionless frequency parameter η and a predefined tolerance *tol*. This tolerance is defined as a percentage of the amplitude A_{max} of the incident wave front, once it arrives at a specified crack edge. This amplitude is chosen such that

$$A_{max} = \max\left(\left|w_A^{inc}\right|, \left|w_B^{inc}\right|\right),$$

where w_A^{inc} and w_B^{inc} are defined in the Appendix. The procedure guarantees that the smallest diffracted wave contained in the solution will have an amplitude smaller or equal to $tol \times A_{max}$. The procedure is listed as follows:

1. Define a value of the dimensionless frequency parameter $\eta = a/\lambda$ and tolerance *tol*.
2. Plot the complex amplitude function
$$A(r) = A_{max} \frac{-\mathrm{e}^{-\mathrm{i}(kr+\pi/4)}}{\sqrt{2\pi kr}} F(2kr) \ ,$$
with
$$k = \frac{2\pi\eta}{a} \ .$$
The function $A(r)$ represents the amplitude of the transfer function of the first order diffraction produced by a plane front interacting with the edges and travelling towards the shadow zone. We have selected the amplitude function for a plane wave front since this wave always contains values greater than those in a cylindrical wave. This is shown later, in Fig. 11. Therefore, if the tolerance is reached for a plane wave, it is also valid for the analogous cylindrical wave. For cases in which $a < r < 2a$, the result corresponds to the second order diffraction. In general, for values where $(n-1)a < r < na$, the result for the amplitude corresponds to the *n*-th order diffraction.
3. From the previous plot, identify the value of *r* for which $A(r) \le tol$.
4. Use this value of *r* to compute *N* as
$$N = \mathrm{int}\left(\frac{r}{a}\right) + 1 \ ,$$
where $\mathrm{int}(\bullet)$ is the integer part function.

The procedure is illustrated in Fig. 3, where we show the variation of $A(r)$ vs *r* for $\eta = 3.0$, $tol = 0.05$, $a = 1.0$ and $A_{max} = 1.0$. The red line indicates the threshold for which tol has already been reached. In this case the obtained number of diffraction orders is $N = 4$. This implies that if the solution is constructed with up to 4-th order diffraction terms, there will not be any diffracted waves with amplitude greater than $0.05A_{max}$.

4. RESULTS

We now validate our current solution to the problem of scattering of *SH* waves by a finite crack constructed by a diffraction based superposition approach. To that end we compared our SBD-solution with results obtained via an integral equation approach based on a direct formulation using the Somigliana identity (*Banerjee and Butterfield, 1981*). The study was conducted in the frequency domain but results are also shown in terms of

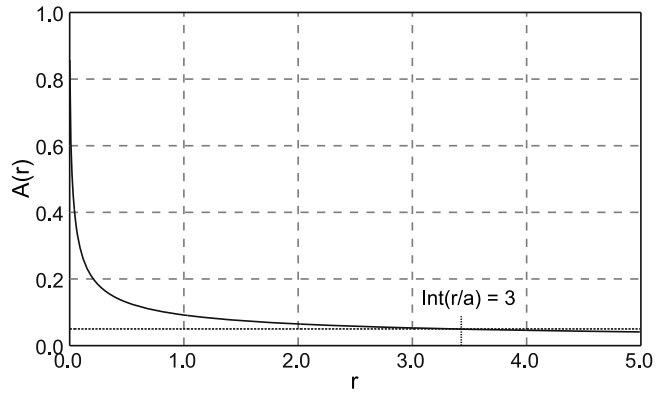

Fig. 3. Variation of the amplitude function $A(r)$ with distance r for a diffracted wave, used to determine the maximum order of diffraction N required in order to reach a specific tolerance *tol* given the dimensionless frequency η.

time histories of relevant response quantities. On the other hand, the validation in the time domain is conducted in terms of synthetic seismograms, for receivers located along the shadow and illuminated zones and in terms of snapshots of the propagation patterns over the complete computational domain for low and high frequency results for incident plane and cylindrical wave fronts. As an additional validation we also compared our results with those obtained by *Sánchez-Sesma and Iturrarán-Viveros (2001)*, where the diffracted waves were assumed to propagate as plane wave fronts neglecting their cylindrical nature. The analyses were first conducted in the frequency domain, where we obtained the transfer functions (*TF*) between the total response and the incident wave. These *TF*s were subsequently fast Fourier transformed in order to derive time domain results after applying a Ricker pulse defined by $f(t) = (2\pi\tau - 1)\mathrm{e}^{-\pi\tau^2}$, where $\tau = f_c(t - t_{ini})$, f_c is central (predominant) frequency (or equivalently in terms of $\eta_c = af_c/\beta$, and t_{ini} is the initial time for the intense phase, i.e. location of the pulse within a general signal. On the other hand, the results at low and high frequencies were obtained with diffraction orders corresponding to $N = 5$ and $N = 3$, respectively. It must be recalled that every additional term in the series implies cylindrical waves emanating from each diffraction source. In this work we considered a crack of unit length, located at $y = [-a/2, a/2]$ (see Fig. 2) and embedded in a homogeneous elastic infinite medium with mass density $\rho = 1.0$ g cm^{-3} and a shear wave propagation velocity $\beta = 1.0$ km s^{-1}.

Figures 4 and 5 show contour maps calculated with the SBD technique for the amplitude of the transfer function for a set of receivers located along the crack surface for a range of values of the dimensionless frequency parameter $\eta = (0, 8]$. The receivers are located along the line $y = [-a/2, a/2]$. Figure 4 corresponds to the results for plane wave incidence while Fig. 5 corresponds to incidence of a cylindrical wave. An interesting result is observed in the SBD solution for the total field associated with the responses for

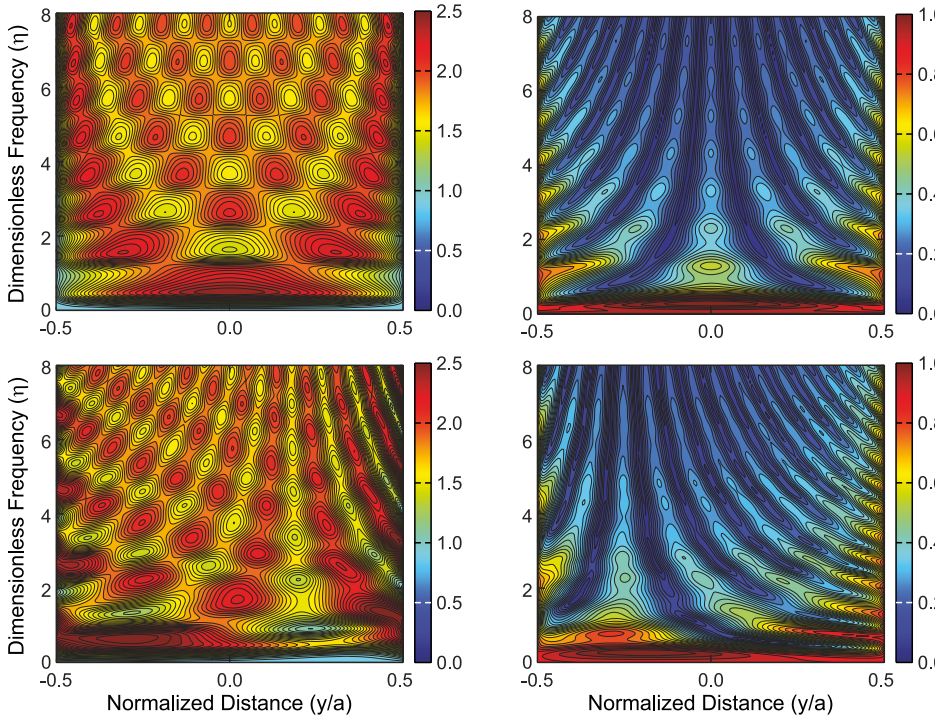

Fig. 4. Frequency domain contour maps for the amplitude of the transfer function for a set of receivers over the crack surface under the plane wave incidence. The results in each row correspond to the solution for incidence angle ϕ_B' of 90° and 120°, respectively while each column corresponds to the illuminated zone (left) and shadow zone (right).

cylindrical and plane wave fronts under normal incidence, and for those for cylindrical and plane wave fronts under an asymmetrical incidence. It is observed that, regardless of the type of incident wave, the response in the shadow zone, consisting only of the contribution from the diffracted field, is very similar in spatial distribution for both the cylindrical and plane wave incidence. Therefore, we can say that the shadow zone response is relatively independent of the type of incident wave. This independence of the response along the shadow zone from the type of incident wave, is the result of the solution over this zone being contributed only by the addition of cylindrical sources located at the edges.

Now, in order to show the convergence properties in our series solution, we display in Fig. 6 the error between the SBD method and the solution based upon the Somigliana representation theorem. For that purpose the same set of contours shown in Figs 4 and 5, have been obtained with the SBD approach and with the representation theorem and compared using the root mean square (*RMS*) error defined by

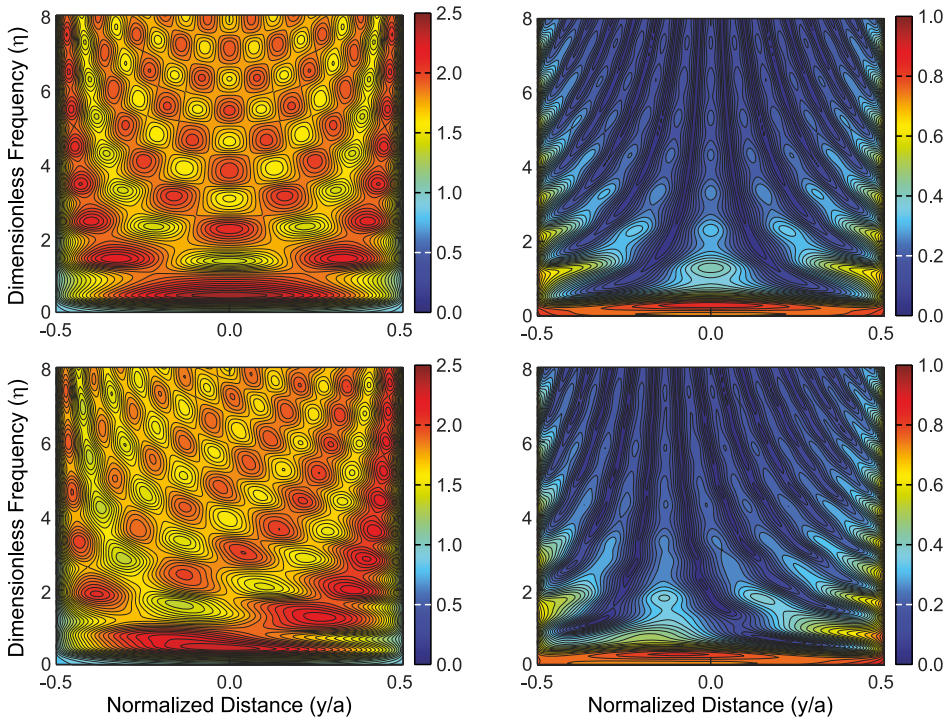

Fig. 5. Frequency domain contour maps for the amplitude of the transfer function for a set of receivers over the crack surface for the cylindrical wave incidence. The first row shows the results in the illuminated zone (left) and shadow zone (right) for $(x_s, y_s) = (-1.0, 0.0)$. The second row corresponds to $(x_s, y_s) = (-1.0, 0.3)$, also in the illuminated zone (left) and shadow zone (right).

$$E_f = \sqrt{\frac{\int \left| TF_f^I - TF_f^{SBD} \right|^2 dx}{\int \left| TF_f^I \right|^2 dx}} ,$$

where TF_f^I is the transfer function computed with integral equation at a frequency f along the crack surface, while TF_f^{SBD} is the equivalent TF computed with the proposed SBD approach. These values correspond to a horizontal cross-section of the TF contours in Figs 4 and 5. This form of describing the error between both solutions allows us to compare the TF at a fixed frequency along the crack surface. Here we compute the error for a dimensionless frequency range $\eta = (0, 8]$ and yielding a curve E_f in dependence of f containing the RMS error for each computed frequency. Since in the SBD-solution the

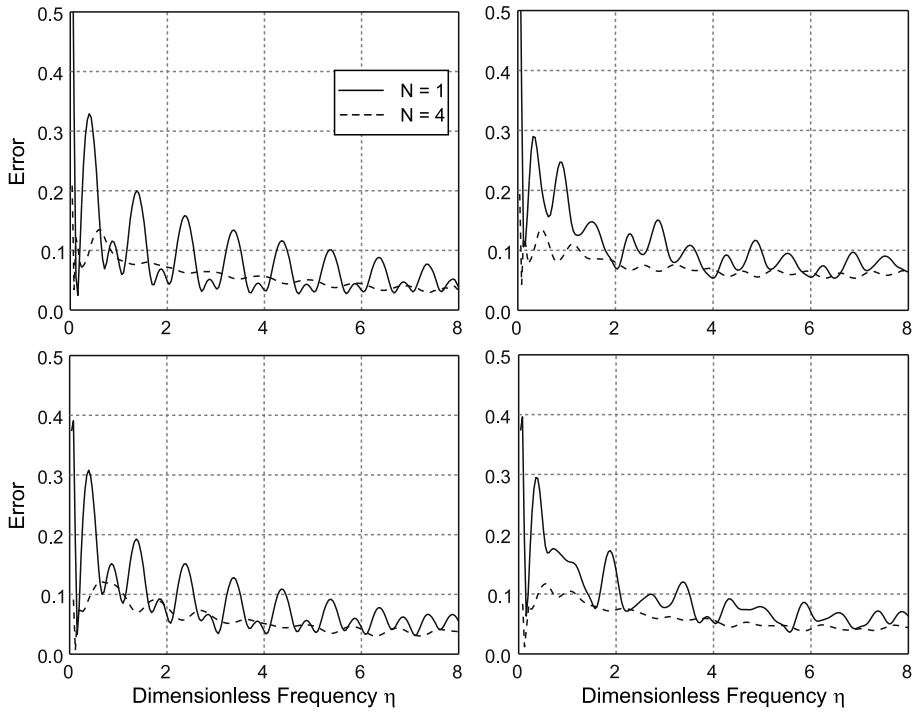

Fig. 6. *RMS* error between the proposed SBD approach and an integral equation based solution. The first row shows the results for plane incidence with incidence angle ϕ'_B of 90° (left) and 120° (right). The second row corresponds to cylindrical wave incidence with source at $(x_S, y_S) = (-1.0, 0.0)$ (left) and $(x_S, y_S) = (-1.0, 0.3)$ (right), respectively. The solid curves correspond to the error after considering only one diffraction term ($N = 1$) in the SBD approach. Similarly the dashed lines represent the error when the SBD solution is obtained considering diffraction up to the 4-th order ($N = 4$).

only approximation is in the diffracted field, we focused on this specific component of the response by studying the transfer functions over the whole frequency range for locations along the crack surface and in the shadow zone. We have excluded the results for the illuminated zone as incident and reflected components are obtained in closed-form and its validation is irrelevant. Results are shown in Fig. 6.

The first row in Fig. 6 displays the *RMS* error curves for plane incidence at $\phi'_B = 90^\circ$ (left) and $\phi'_B = 120^\circ$ (right), while the second row displays the error for cylindrical incidence with a line source located at $(x_S, y_S) = (-1.0, 0.0)$ (left) and $(x_S, y_S) = (-1.0, 0.3)$ (right). In all of these plots, the curves represent the *RMS* error between the SBD and the reference solution, i.e. the integral equation based solution. We show the errors corresponding to $N = 1$ and $N = 4$. As expected, the results neglecting the

interaction between the crack edges, corresponding to a single diffraction term and represented by the solid line, exhibit large differences with respect to the integral approach. This difference is stronger in the low frequency regime since at those frequencies the amplitude of the first diffracted wave is still very large and it requires several higher order interactions before their contribution can be neglected. However, it is interesting to observe how at high frequencies a good approximation is obtained by the SBD method even with a single diffraction order. This low level of interaction between the two diffraction sources at high frequencies, is evident from the $1/\sqrt{kr}$ decay present in Eq. (1). On the other hand, when 4-th order diffraction is considered in the SBD solution, accuracy is maintained at high and low frequencies.

Figure 7 displays snapshots of the propagation patterns for the case of plane waves incident with $\phi_B' = 90^\circ$ and $\phi_B' = 120^\circ$ over computational domains of size $10a \times 10a$ and $3a \times 3a$. The excitation in each case is a Ricker pulse with low and high characteristic frequencies and with an SBD-solution obtained with diffractions of 5-th and 3-rd order for the low and high frequency computations respectively. Each frame in the figure, qualitatively compares the results obtained with the SBD approach (left) and those from the integral equation based approach (right) at different instants of time. Although these comparisons in the time domain are highly qualitative, several observations indicating the validity of the SBD technique can be made. For instance, in every case, and as a result of the interaction between the edges of the crack, cylindrical wave fronts emanating from each diffraction source can be observed after the advancement of the incident front. It is also observed how the incident wave front is progressively recovered over the shadow zone of the incident rays. This recovery is completely achieved due to the contribution from the diffracted field. Moreover, this observation, regarding the recovery effect of the diffracted part of the response, is especially evident in the low frequency regime, where intuitively it should take place at shorter distances from the crack. Theoretically, at $t = \infty$ the main wave front should be fully recovered whereas the reflected wave should have completely vanished, also as a result of the diffracted component.

The same set of analyses was conducted for the case of incident cylindrical waves. The comparison in terms of snapshots of the propagation patterns computed with both methods are displayed in Fig. 8 for the same domains used in the case of plane wave incidence. The sources for the cylindrical waves were located at the positions $(x_s, y_s) = (-2.0, 0.3)$ and $(x_s, y_s) = (-1.0, 0.3)$ in order to introduce asymmetric conditions into the problem. As in the case of incident plane waves, at high frequencies it is observed how the diffracted field exhibits negligible values once it reaches the opposite edge of the crack yielding good results with only 3 orders of diffraction considered in the series. Similarly, the results also reveal the property of the diffracted field of restoring continuity of the solution over the shadow zone.

Figure 9 shows synthetic seismograms for receivers located in the illuminated and shadowed surface of the crack under plane wave incidence computed with the SBD and the integral equation. The results from the SBD technique and the integral equation solution have been superimposed. It is observed that the SBD method predicts results in good agreement with the integral equation when the considered diffractions are only of

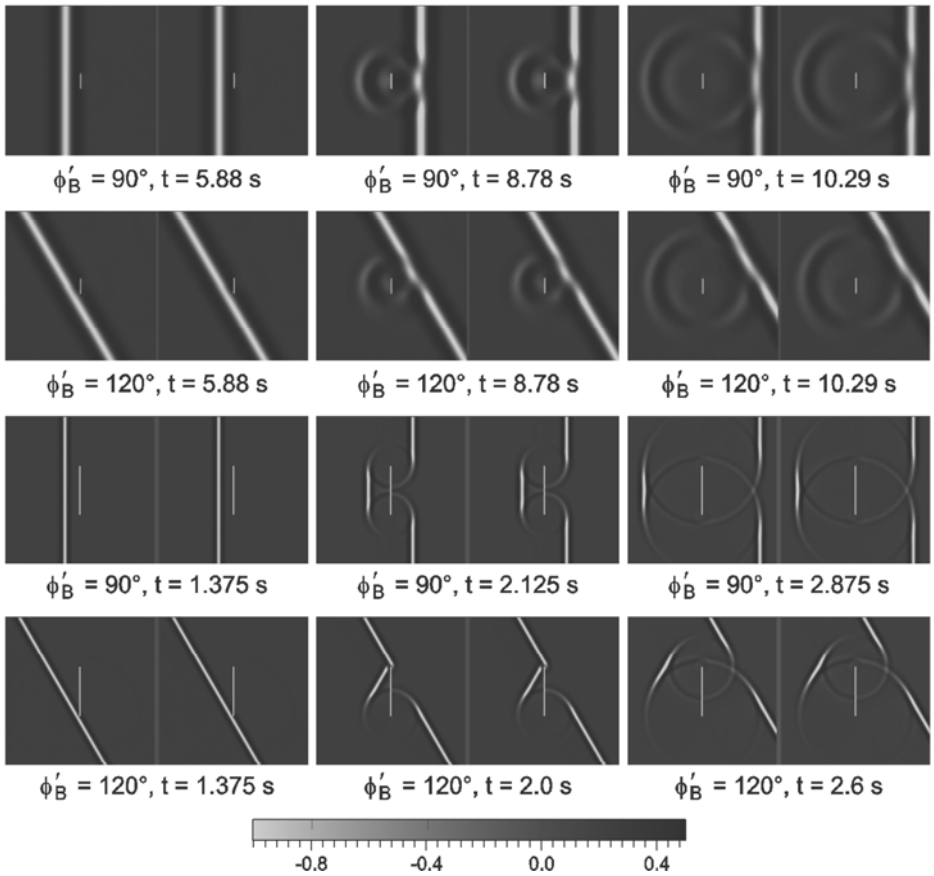

Fig. 7. Snapshots of the propagation patterns for a single crack subjected to an incident plane wave in the form of a Ricker pulse obtained with the current SBD method (left) and the integral equation based solution (right). The first two rows correspond to a characteristic dimensionless frequency of the pulse $\eta_c = 0.5$ for incident angles $\phi'_B = 90^\circ$ and 120°, while the last two rows correspond to a characteristic dimensionless frequency of the pulse $\eta_c = 5.0$ and the incidence angles $\phi'_B = 90^\circ$ and 120°.

5-th ($\eta = 0.5$) and 3-rd ($\eta = 5.0$) orders. The same response is observed from the synthetic seismograms and time histories displayed in Fig. 10 for cylindrical wave incidence.

As an additional validation we compare in Fig. 11 our results with those reported by *Sánchez-Sesma and Iturrarán-Viveros (2001)*. In order to test the level of error introduced by that plane wave assumption, these authors compared their results with those obtained from the recursive application of the solution for a generalized wedge formulated in *MacDonald (1902)*. These authors showed how their solution method, which is based on the solution by *Sommerfeld (1896)*, loses accuracy in the low frequency regime due to the

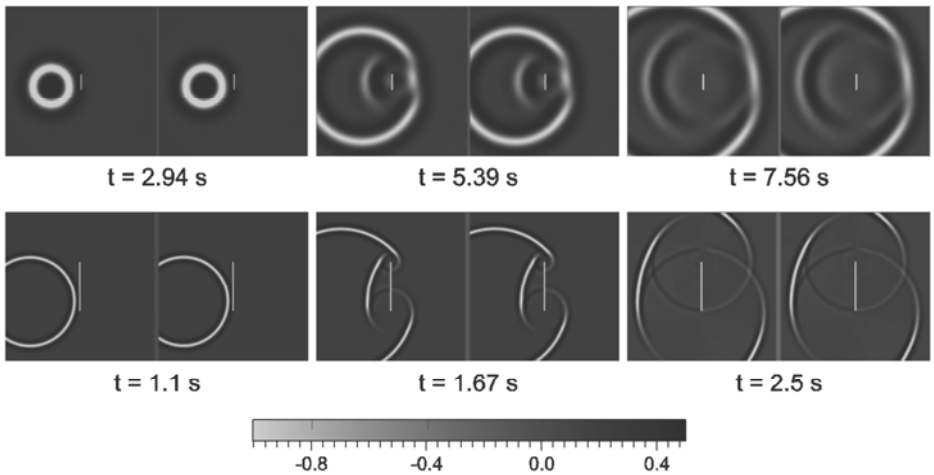

Fig. 8. Snapshots of the propagation patterns for a single crack as the result of an incident cylindrical wave in the form of a Ricker pulse obtained with the current SBD method (left) and the integral equation based solution (right). At the low frequency regime the pulse is characterized by its central frequency $\eta_c = 0.5$, a total time window of $t_{tot} = 13.0$ s and initial time $t_{ini} = 2.0$ s. The sources were located at $(x_s, y_s) = (-2.0, 0.3)$ (first row). At the high frequency regime the pulse had a central frequency $\eta_c = 5.0$, a total time window $t_{tot} = 4.2$ s and initial time $t_{ini} = 0.2$ s with source located at $(x_s, y_s) = (-1.0, 0.3)$ (second row).

plane wave approximation used for the higher order diffracted waves. Here we compare our results with those from *Sánchez-Sesma and Iturrarán-Viveros (2001)*. In the plot we used the same notation as in *Sánchez-Sesma and Iturrarán-Viveros (2001)*, where r represents the radial coordinate of any point along the illuminated zone of the crack and r_0 is the location of a source point in the shadow zone of the crack, i.e. $r_0 = a$. In the plot we describe the behaviour of the amplitude of the transfer function for a diffracted wave travelling along the illuminated zone produced by a plane or cylindrical wave travelling along the shadow zone. The comparison corresponds to 4 different dimensionless frequencies, namely $\kappa r_0 = \pi/2$, π, 2π, 3π. The good agreement between the results from the SBD technique and the solution from *Sánchez-Sesma and Iturrarán-Viveros (2001)*, at high and low frequency values is clearly observable. Note that at low frequencies, when we assume the diffracted waves predicted by the SBD technique as plane fronts, we obtain results which are in agreement with those reported by *Sánchez-Sesma and Iturrarán-Viveros (2001)*, whereas the same results depart from those obtained with the exact cylindrical front representation.

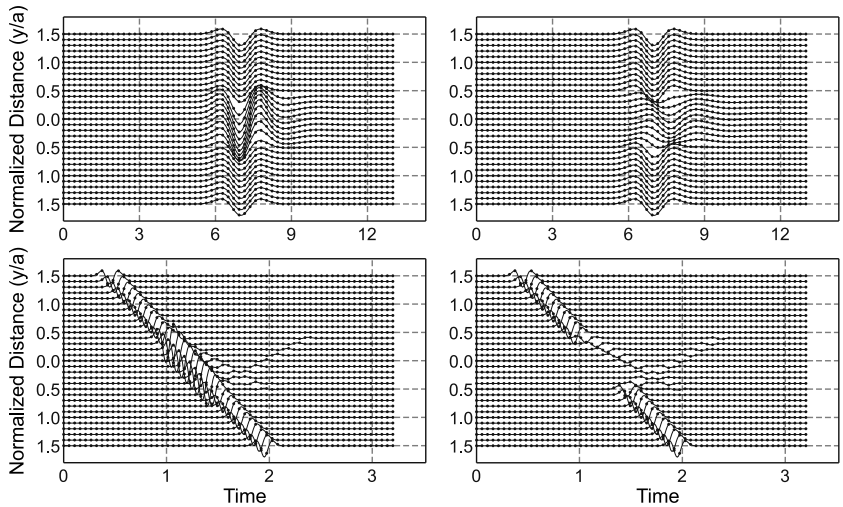

Fig. 9. Synthetic seismograms for receivers over the illuminated (left) and shadowed (right) crack surface for an incident plane wave in the form of a Ricker pulse with high and low central frequencies obtained with the SBD technique (dots) and the integral equation based algorithm (curves). The results in row 1 are for a pulse defined by $\eta_c = 0.5$, $t_{tot} = 13.0$ s, $t_{ini} = 7.0$ s and those in row 2 are for a pulse defined by $\eta_c = 5.0$, $t_{tot} = 3.2$ s and $t_{ini} = 1.2$ s. The results were obtained with 5-th and 3-rd order diffraction terms.

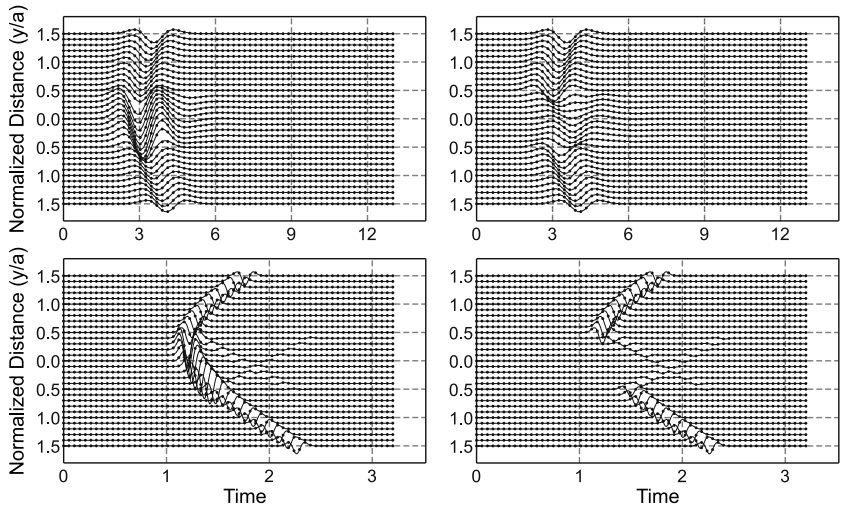

Fig. 10. The same as in Fig. 9, but the results in row 1 are for a pulse defined by $\eta_c = 0.5$, $t_{tot} = 13.0$ s, $t_{ini} = 2.0$ s and those in row 2 are for a pulse defined by $\eta_c = 5.0$, $t_{tot} = 3.2$ s and $t_{ini} = 0.2$ s. The results were obtained with 5-th and 3-rd order diffraction terms and the source was located at $(x_s, y_s) = (-1.0, 0.3)$.

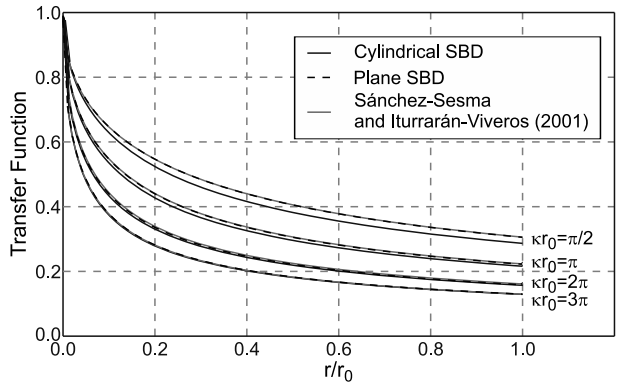

Fig. 11. Comparison between the results from the SBD technique and those obtained with the solution by *Sánchez-Sesma and Iturrarán-Viveros (2001)*. SBD - superposition-based diffraction, r - radial coordinate to the field point measured from the vertex of the wedge, κr_0 - dimensionless frequency.

5. CONCLUSIONS

A series solution to the scattering of plane and cylindrical horizontally polarized *SH* shear waves incident upon a crack of finite length embedded in a full-space was constructed. The solution was obtained using the superposition of incident, reflected and diffracted rays. This last term in the total field was calculated using the canonical solution for the diffraction of electromagnetic waves by the edge of an infinite wedge due to *Kouyoumjian and Pathak (1974)* and its generalized form by *Jaramillo et al. (2013)*. The complete diffracted field for the finite crack, was built through the superposition of two opposite infinite wedges. The solution is shown to be general enough as it is valid for plane waves incident at arbitrary angles and for cylindrical waves with sources at arbitrary locations. On the other hand, in the proposed solution, the waves diffracted by the edges of the crack are propagated onto the opposite edge as cylindrical fronts yielding an accurate solution at the low and high frequency regime. In contrast to alternative solutions available in the literature and represented as series of infinite terms, where accuracy is treated in terms of the convergence of the series, in our method accuracy is related to physically based diffraction sources in terms of higher order diffraction contributions. As such, it is controlled on a physical basis by the number of required terms shown to depend upon the frequency content of the incident wave. Moreover, the near and far field solution for the total displacement field is calculated with the same expression, eliminating the need to use an independent application of the representation theorem like in alternative solutions. At high frequencies only a small number of terms is needed since the amplitude of the diffracted waves dies off with distance reaching a vanishing value as it interacts with the opposite corner. Also, since in the shown solution the incident and reflected rays are represented in closed-form, as opposed to solutions based on separation of variables where the whole field is represented by an infinite series, the solution can be constructed

to a desired accuracy with only the consideration of a few terms. Moreover, we propose an empirical rule to obtain the number of terms required to obtain a solution within a specific tolerance depending on a dimensionless frequency. On the other hand, for the particular case of normal incidence, the solution is reduced to a single expression which is found after taking advantage of the symmetry of the problem. Due to the low computational cost involved in the evaluation of the different terms in the series and to their physical nature, this solution is very appealing for use in the validation of numerical implementations. Finally, a comparison between the results for plane wave incidence and those for a cylindrical wave reveal that the diffracted field in the shadow zone is independent of the type of incident wave.

Acknowledgements: This work was supported by Colciencias-EAFIT under the Jovenes Investigadores program.

APPENDIX

Function $G(\phi_A, \phi'_A, r_A, L_A)$ for a general incidence

The function $G(\ )$ required for the evaluation of the diffraction contribution in Eq. (6) has the form

$$G(\phi_A, \phi'_A, r_A, L_A) = \frac{-\mathrm{e}^{-\mathrm{i}(kr+\pi/4)}}{4\sqrt{2\pi kr}} \left[\cot\left(\frac{\pi+(\phi-\phi')}{4}\right) F\left(kLb^{+}(\phi-\phi')\right) \right.$$
$$+\cot\left(\frac{\pi-(\phi-\phi')}{4}\right) F\left(kLb^{-}(\phi-\phi')\right) + \cot\left(\frac{\pi+(\phi+\phi')}{4}\right) F\left(kLb^{+}(\phi+\phi')\right)$$
$$\left. +\cot\left(\frac{\pi-(\phi+\phi')}{4}\right) F\left(kLb^{-}(\phi+\phi')\right) \right],$$

with $L_\bullet$ given by

$$L_\bullet = \begin{cases} r_\bullet & \text{if } n=1, \text{ and plane wave incidence}, \\ \dfrac{r_\bullet r'_\bullet}{r_\bullet + r'_\bullet} & \text{if } n=1, \text{ and cylindrical wave incidence}, \\ \dfrac{r_\bullet a}{r_\bullet + a} & \text{other case}. \end{cases}$$

In the above, the subscript $\bullet$ may take the specific values A or B depending on the crack edges. Accordingly in Eq. (6) $\phi_\bullet$ and $r_\bullet$ represent the angular and radial coordinates of a field point measured with respect to the edges A and B, $r'_\bullet$ is the radius of the incident cylindrical wave also measured from each edge. $w_\bullet^{inc}$ is the complex amplitude of the incident front upon arrival at a given crack edge. The parameter N indicates the number of

terms considered in the series. The contributions from the incident fronts at the edges are given by

$$\text{Plane incident wave}\begin{cases} w_A^{inc} = w^{inc}\mathrm{e}^{\mathrm{i}ka\cos(\phi'_A)/2}, \\ w_B^{inc} = w^{inc}\mathrm{e}^{\mathrm{i}ka\cos(\phi'_B)/2}, \end{cases}$$

$$\text{Cylindrical incident wave}\begin{cases} w_A^{inc} = w^{inc}\mathrm{e}^{\mathrm{i}kr'_A}, \\ w_B^{inc} = w^{inc}\mathrm{e}^{\mathrm{i}kr'_B}. \end{cases}$$

On the other hand, the terms V_A and V_B are given by

$$V_{A,B} = \begin{cases} 1.0 & \text{if } n = 1, \\ G\left(0.0, 0.0, na, L_{A,B}\right) & \text{if } n > 1. \end{cases}$$

Function $G(\phi, \pi/2, r, L)$ for normal incidence

The function $G(\ )$ required for the evaluation of the diffraction contribution in the case of normal incidence has the form

$$G(\phi, \pi/2, r, L) = \frac{-\mathrm{e}^{-\mathrm{i}(kr+\pi/4)}}{4\sqrt{2\pi kr}}\left[\cot\left(\frac{\frac{\pi}{2}+\phi}{4}\right)F\left(kLb^{+}\left(\phi-\frac{\pi}{2}\right)\right)\right.$$
$$+\cot\left(\frac{\frac{3\pi}{2}-\phi}{4}\right)F\left(kLb^{-}\left(\phi-\frac{\pi}{2}\right)\right)+\cot\left(\frac{\frac{3\pi}{2}+\phi}{4}\right)F\left(kLb^{+}\left(\phi+\frac{\pi}{2}\right)\right)$$
$$\left.+\cot\left(\frac{\frac{\pi}{2}-\phi}{4}\right)F\left(kLb^{-}\left(\phi+\frac{\pi}{2}\right)\right)\right],$$

with

$$L_{\bullet} = \begin{cases} r_{\bullet} & \text{if } n = 1, \\ \dfrac{r_{\bullet}a}{r_{\bullet}+a} & \text{if } n > 1. \end{cases}$$

References

Abo-Zena A. and King C., 1973. SH pulse in an elastic wedge. *Bull. Seismol. Soc. Amer.*, **63**, 1571–1582.

Achenbach J.D., Gautesen A.K. and McMaken H., 1982. *Ray Methods for Waves in Elastic Solids: with Applications to Scattering by Cracks*. Pitman Advanced Publishing Program, Boston/London/Melbourne.

Banerjee P.K. and Butterfield R., 1981. *Boundary Element Methods in Engineering Science*. McGraw-Hill Book Co., London, U.K.

Caleap M., Aristegui C. and Angel Y.C., 2007. Further results for antiplane scattering by a thin strip. *J. Acoust. Soc. Am.*, **122**, 1876–1879.

Chen B.J., Du C.L., Zhang J.L. and Xiao Z.M., 2013. Scattering of sh waves by an arbitrarily orientated closed crack. *Acta Mech.*, **224**, 2649–2662.

Chen T., Fehler M., Fang X., Shang X. and Burns D., 2012. Sh wave scattering from 2-d fractures using boundary element method with linear slip boundary condition. *Geophys. J. Int.*, **188**, 371–380.

De Hoop A. T., 2000. Transient two-dimensional kirchhoff diffraction of a plane elastic sh wave by a generalized linear-slip fracture. *Geophys. J. Int.*, **143**, 319–327.

Garnier C., Pastor M.-L., Eyma F. and Lorrain B., 2011. The detection of aeronautical defects in situ on composite structures using non destructive testing. *Compos. Struct.*, **93**, 1328–1336.

Hudson J., 1963. SH waves in a wedge-shaped medium. *Geophys. J. R. Astron. Soc.*, **7**, 517–546.

Iturrarán-Viveros U., Vai R. and Sánchez-Sesma F.J., 2005. Scattering of elastic waves by a 2-D crack using the indirect boundary element method (IBEM). *Geophys. J. Int.*, **162**, 927–934.

Iturrarán-Viveros U., Vai R. and Sánchez-Sesma F.J., 2010. Diffraction of sh cylindrical waves by a finite crack: an analytical solution. *Geophys. J. Int.*, **181**, 1634–1642.

Jaramillo J., Gomez J., Saenz M. and Vergara J., 2013. Analytic approximation to the scattering of antiplane shear waves by free surfaces of arbitrary shape via superposition of incident, reflected and diffracted rays. *Geophys. J. Int.*, **192**, 1132–1143.

Keller J., 1956. Diffraction by a convex cylinder. *IEEE Trans. Antenn. Propag.*, **AP-24**, 312–321.

Keller J., 1957. Diffraction by an aperture. *J. Appl. Phys.*, **28**, 426–444.

Keller J., 1962. Geometrical theory of diffraction. *J. Opt. Soc. Am.*, **52**, 116–130.

Kouyoumjian R. and Pathak P., 1974. A uniform geometrical theory of diffraction for an edge in a perfectly conducting surface. *Proc. IEEE*, **62**, 1448–1461.

Krüger O.S., Saenger E.H. and Shapiro S.A., 2005. Scattering and diffraction by a single crack: an accuracy analysis of the rotated staggered grid. *Geophys. J. Int.*, **162**, 25–31.

MacDonald H., 1902. *Electric Waves*. Cambridge University Press, Cambridge, U.K.

Mow C.-C. and Pao Y.-H., 1971. The diffraction of elastic waves and dynamic stress concentrations. The Rand Corporation, Santa Monica, CA (https://www.rand.org /content/dam/rand/pubs/reports/2007/R482.pdf).

Murai Y., 2007. Scattering attenuation, dispersion and reflection of sh waves in two-dimensional elastic media with densely distributed cracks. *Geophys. J. Int.*, **168**, 211–223.

Perez-Ruiz J., Luzon F. and Garca-Jerez A., 2007. Scattering of elastic waves in cracked media using a finite difference method. *Stud. Geophys. Geod.*, **51**, 59–88.

Sánchez-Sesma F.J. and Iturrarán-Viveros, U., 2001. Scattering and diffraction of sh waves by a finite crack: an analytical solution. *Geophys. J. Int.*, **145**, 749–758.

Sommerfeld A., 1896. Mathematische theorie der diffraktion. *Math. Ann.*, **47**, 317–374 (in German).

Tsaur D., 2010. Exact scattering and diffraction of antiplane shear waves by a vertical edge crack. *Geophys. J. Int.*, **181**, 1655–1664.

Waterman P.C. and Truell R., 1961. Multiple scattering of waves. *J. Math. Phys.*, **2**, 512–537.